NASA TECHNICAL MEMORANDUM

NASA TM X-62,494

NASA TM X-62,494

OPTIMAL CONTROL ALLEVIATION OF TILTING PROPROTOR GUST RESPONSE

Wayne Johnson

Ames Research Center
and
U.S. Army Air Mobility R&D Laboratory
Moffett Field, Calif. 94035

October 1975

1. Report No.	2. Government Accession No.	3. Recipient's Catalog No.
TM X-62,494		

4. Title and Subtitle	5. Report Date
OPTIMAL CONTROL ALLEVIATION OF TILTING PROPPROTOR GUST RESPONSE	6. Performing Organization Code

7. Author(s)	8. Performing Organization Report No
Wayne Johnson	A-6307

9. Performing Organization Name and Address	10. Work Unit No.
NASA Ames Research Center and U.S. Army Air Mobility R&D Laboratory Moffett Field, California 94035	11. Contract or Grant No.

12. Sponsoring Agency Name and Address	13. Type of Report and Period Covered
National Aeronautics and Space Administration Washington, D. C. 20546	Technical Memorandum
	14. Sponsoring Agency Code

15. Supplementary Notes

16. Abstract

Optimal control theory is applied to the design of a control system for alleviation of the gust response of tilting proprotor aircraft. Using a proprotor and cantilever wing analytical model, the uncontrolled and controlled gust response is examined over the entire operating range of the aircraft except for hover: helicopter mode, conversion, and airplane mode flight. Substantial improvements in the loads, ride quality, and aeroelastic stability are possible with a properly designed controller. A single controller, nominally optimal only at the design point speed (160 knots here), operated efficiently over the entire speed range, with the possible exception of very low speed in helicopter mode. Kalman-Bucy filters were used as compensation networks to provide state estimates from various measurements in the wing motion, rotor speed perturbation, and tip-path-plane tilt.

17. Key Words (Suggested by Author(s))	18. Distribution Statement
Optimal control Tiltrotor aircraft Gust alleviation	Unlimited STAR Category - 01

19. Security Classif. (of this report)	20. Security Classif. (of this page)	21. No. of Pages	22. Price*
Unclassified	Unclassified	26	$3.75

*For sale by the National Technical Information Service, Springfield, Virginia 22151

OPTIMAL CONTROL ALLEVIATION OF TILTING PROPROTOR GUST RESPONSE

Wayne Johnson

Ames Research Center
and
U.S. Army Air Mobility R&D Laboratory

ABSTRACT

Optimal control theory is applied to the design of a control system for alleviation of the gust response of tilting proprotor aircraft. Using a proprotor and cantilever wing analytical model, the uncontrolled and controlled gust response is examined over the entire operating range of the aircraft except for hover: helicopter mode, conversion, and airplane mode flight. Substantial improvements in the loads, ride quality, and aeroelastic stability are possible with a properly designed controller. A single controller, nominally optimal only at the design point speed (160 knots here), operated efficiently over the entire speed range, with the possible exception of very low speed in helicopter mode. Kalman-Bucy filters were used as compensation networks to provide state estimates from various measurements in the system. Efficient control requires the measurement of the wing motion, rotor speed perturbation, and tip-path-plane tilt.

INTRODUCTION

The tilting proprotor aircraft is a promising concept for short haul, V/STOL missions. The successful operation of this aircraft will require an acceptable level of loads and ride quality in response to atmospheric turbulence. Small V/STOL aircraft operating at low altitudes will be expected by users to have ride qualities at least as good as current large jet-transport aircraft.

A number of studies have established the influence of gust response on the design of tilting proprotor aircraft. A representative proprotor design encounters design limit blade loads due to vertical gusts in high speed airplace mode flight, and design limit drive train loads due to asymmetric longitudinal gusts (ref. 1). The cabin acceleration response to vertical gusts has been found to be about the same as that of a conventional aircraft of similar size (a higher wing loading offsetting the proprotor effects), while the response to lateral and longitudinal turbulence is somewhat higher than for a conventional turboprop aircraft (ref. 2). It is concluded therefore that some ride quality improvement will be required for extensive utilization of the tilting proprotor aircraft on V/STOL missions. Another interesting factor is that design variations to reduce tiltrotor noise tend to increase

the gust response. One study has shown a 50% increase in the vertical acceleration due to vertical gusts in cruise, for a 5 PNdB noise reduction (ref.3).

We wish to consider the design of a feedback control system for alleviation of tilting proprotor aircraft gust response. The primary interest at this stage is in what improvement of the loads and ride quality is feasible with a properly designed controller, and the characteristics of the measurements and control required to achieve it. Optimal control theory will be used to design a gust alleviation system. A Kalman-Bucy filter will be used as a compensation network to provide a state estimation from various measurements. The report begins with a discussion of the analytical model for the proprotor dynamic behavior. Then the control design process will be briefly discussed. Finally the results for the uncontrolled and controlled gust response of a tilting proprotor will be examined over the entire range of operation: helicopter mode, conversion, and airplane cruise mode flight.

PROPROTOR MODEL

An analytical model has been developed for the aeroelastic behavior of a tilting proprotor and cantilever wing (refs. 4 and 5). The dynamic system is described by a set of linear differential equations. This model has been applied (in ref. 6) to the dynamics of two full-scale proprotor designs: a gimballed, stiff-inplane rotor and a hingeless, soft-inplane rotor. The uncontrolled dynamic stability and aeroelastic behavior was investigated (ref. 6), including a consideration of what elements of the analytical model are required for an adequate representation of the dynamics, and a comparison with the results of full-scale tests. These studies (refs. 5 and 6) have concluded that the rotor model required for an analysis of proprotor dynamics consists of the following degrees of freedom: the first two bending modes per blade (first out-of-plane mode and first inplane mode); gimbal pitch and yaw for a gimballed rotor; and the rotor speed perturbation, including engine inertia and damping effects. The rotor blade pitch motion was found to have a significant role in the dynamics. For control investigations however, it is important to keep the order of the system as low as possible. Thus the blade pitch dynamics are included by using a quasistatic model, which does not add degrees of freedom to the system. The quasistatic torsion representation has been shown to be an adequate model for the flight conditions considered here (ref. 6).

The rotor speed perturbation ($\dot{\psi}_s$) has an important role in the dynamics of tilting proprotor aircraft (refs. 5 and 6). With a turboshaft engine the rotor behaves nearly as if windmilling as far as its dynamic behavior is concerned. The engine inertia and damping are included in the ψ_s dynamics, since they do have some influence (ref. 5). A rotor speed governor is also included, consisting of integral feedback of the rotor speed error measured with respect to the pylon, to rotor collective pitch, with a small lead in helicopter mode to increase the damping of the rotor rotational motion. The governor has a very long time constant however, so it does not have much influence on the dynamics (ref. 5). The rotor model used is valid for high

and low inflow, and for axial and nonaxial flight. Hence it is applicable to the entire range of proprotor operation: helicopter, conversion, and airplane cruise modes. In nonaxial flow a constant coefficient approximation is used for the equations of motion. This is a good representation of tilting proprotor dynamics in helicopter forward flight and conversion because of the low advance ratio characteristic of the operation of this aircraft (ref. 6).

The proprotor and cantilever wing configuration contains the basic features of the tilting proprotor aircraft aeroelastic behavior, specifically the high inflow aerodynamics of the rotor and the coupling of the rotor and elastic wing motion. In addition this model is simpler, and most importantly of lower order than a complete aircraft model. Hence it is appropriate for an initial investigation of the optimal control alleviation of proprotor gust response. Investigation of the response and control system design for an actual proprotor aircraft would of course require replacement of the cantilever wing by a more complete support model. For the wing motion we consider the three lowest frequency degrees of freedom: first mode vertical bending, first mode chordwise bending, and first mode torsion.

For controls the rotor collective and cyclic pitch (both axes of cyclic), and a wing flaperon are considered. The flaperon control is a 30% chord trailing edge control surface extending over the outer 50% of the span of the wing. We consider three components of aerodynamic gust: longitudinal, lateral, and vertical. The three components are assumed to be independent, and each is uniform throughout space.

The control system analysis will be applied here primarily to a gimballed, stiff-inplane rotor. A complete description of this rotor and wing is given in reference 6. The rotor has three blades, of radius 3.81 m. The flap frequency is nearly $\nu_\beta = 1$/rev (the rotor does have a weak hub spring, and positive pitch/flap coupling); and the lag frequency is $\nu_\zeta = 1.2$ to 1.5/rev, depending on the collective pitch and rotor speed. The wing has natural frequencies of .42/rev in vertical bending and .70/rev in chordwise bending (at cruise mode rotor speed), which are typical of tilting proprotor aircraft. A hingeless rotor design will also be considered, in order to examine the influence of the rotor type on the gust response and control design.

In summary, the proprotor and wing model used in the present analysis consists of the following degrees of freedom: rotor gimbal pitch and yaw tilt, rotor coning (β_0, a blade elastic bending mode), two cyclic lag modes (giving respectively lateral and vertical displacement of the net rotor center of gravity), and the rotor rotational speed perturbation $\dot{\psi}_s$; and the wing vertical bending, chordwise bending, and wing torsion. There are a total of nine second-order degrees of freedom, hence 18 states in the system. There are four controls: rotor collective, lateral cyclic, and longitudinal cyclic pitch; and wing flaperon. Finally the three gust components are the external disturbance of the system.

CONTROL SYSTEM DESIGN

Optimal Controller

Optimal control theory will be used to design a gust alleviation system. The theory constructs a feedback controller for a linear system, to minimize a quadratic performance index (ref. 7). Consider a linear, time-invariant system (i.e., the proprotor and wing). Let x be the vector of the system states (degrees of freedom), u the vector of controls, and g the vector of gust components. The system is described by a set of constant coefficient, linear differential equations:

$$\dot{x} = Fx + Gu + Dg$$

where F, G, and D are constant matrices. Define the quadratic performance index as follows:

$$J = \int_0^\infty \left(x^T Ax + u^T Bu\right) dt$$

where A is a constant, symmetric, and nonnegative definite matrix; and B is constant, symmetric, positive definite. Only the case where A and B are also diagonal is considered. The control problem is to find a control law for u to minimize the performance index for arbitrary excitation of the system by the gust disturbance. The solution is the optimal deterministic controller (ref. 7), which is linear state variable feedback, $u = -Cx$, where $C = B^{-1}G^TS$, and S is the constant, symmetric, positive definite matrix solution of the Ricatti equation

$$SF + F^TS - SGB^{-1}G^TS + A = 0$$

The Ricatti equation is solved by Potter's method (ref. 8).

The diagonal elements of the weighting matrices A and B may be interpreted as $(x_{max})^{-2}$ and $(u_{max})^{-2}$ respectively (ref. 6). Only the relative magnitudes of the weights in the performance index are important, since any common factor simply scales J. Based on the solution for a first order system, we may interpret $(A/B)^{1/2}$ as the "gain" of the system, which determines the level of the feedback control. No weight is placed in A on those states corresponding to the velocities of the degrees of freedom; it is sufficient to constrain the displacement (adding a constraint on the velocities may be done with a single additional parameter, representing the frequency content of the allowable motion). In summary, A and B are diagonal, with no constraint in A on the velocities of degrees of freedom. The remaining elements of the weighting matrices are chosen so the rms acceleration of the wing and rotor motion have about the same percent reduction at high gain. For the gimballed rotor, a weight of 0.1 rad^{-2} was used for the rotor flap, lag, and ψ_g degrees of freedom; a weight of 1.0 for the rotor coning and the wing degrees of freedom; and a weight of $(gain)^{-2}$ for the controls (B). For most of the results presented here a gain of 10 was used.

State Estimation

To design a compensation network we consider a Kalman-Bucy filter to estimate the states from various measurements. The control problem is as defined above, except that we no longer assume perfect knowledge of the system states for the feedback law. Now a limited number of noisy measurements are considered. Let z be the vector of the measurements, $z = Hx + v$, where H is a constant matrix; and v is stationary, white, Gaussian measurement noise, with zero mean and a covariance $E[v(t)v^T(\tau)] = R\delta(t - \tau)$. R is a constant, symmetric, positive definite correlation matrix. The control problem is to find the control law for u which minimizes the expected value of the performance index for a system with measurement and process noise. The process noise in this case is the aerodynamic gust disturbance (discussed below). The solution is the optimal controller together with the states estimated by a Kalman-Bucy filter (ref. 6). Thus we have linear feedback, $u = -Cx_e$, where C is the same matrix as the optimal deterministic controller above, and x_e is the estimate of the state which must be obtained from the measurements z. The Kalman-Bucy filter gives a maximum likelihood/minimum variance estimate of the state:

$$\dot{x}_e = Fx_e + Gu - K(z - Hx_e)$$

where $K = -PH^TR^{-1}$ and P is the solution of the matrix Ricatti equation

$$FP + PF^T - PH^TR^{-1}HP + DQD^T = 0$$

Q is the correlation matrix of the process noise (the gust). For the measurement noise, it is assumed that R is diagonal with elements equal to $(10^6\Omega)^{-1}$ sec; this corresponds to broadband noise with say a level of .07 deg rms and a 3/rev break frequency.

Gust Model

The Kalman-Bucy filter assumes white process noise. The aerodynamic gust is not well represented by a constant spectrum however, rather the gust strength is concentrated at low frequencies. A Markov-process gust model is used to obtain the appropriate gust spectrum (ref. 9). The vector of the three gust components is g; let

$$\dot{g} = -\frac{1}{\tau_G} g + w$$

where τ_G is the correlation time of the gust; and w is stationary, white, Gaussian noise with zero mean and a correlation $E[w(t)w^T(\tau)] = Q_G\ \delta(t - \tau)$. Q_G is a constant, symmetric, non-negative definite matrix. It is assumed that Q_G is diagonal, with all elements equal to $2\sigma_G^2/\tau_G$.

Hence the gust velocity is a Markov process. The three components are uncorrelated, with identical statistics. Each component of g has zero mean and a covariance $E(g^2) = (1/2)Q_G\tau_G = \sigma_G^2$. So σ_G is the rms level of the gust

velocity. The gust spectrum is

$$S_G = \frac{\sigma_G{}^2 \tau_G}{\pi} \frac{1}{1 + (\tau_G \omega)^2}$$

Thus the gust velocities are included in the state vector, and the first order equations for g to the system differential equations. The process noise for the resulting system is w (which directly excites only the gust velocities); w is white noise, as the analysis requires. Although g is added to the system states, there can of course be no constraint on the gust in the performance index (i.e., in the matrix A). The control matrix C includes feedback of the gust components now, but it is found here that they are small; in any case, the elements in C corresponding to the actual system degrees of freedom are independent of the inclusion of the gust model.

The above gust spectrum compares well with the more usual von Kármán spectrum. We identify τ_G by matching to the von Kármán spectrum at frequency $\omega = 0$, obtaining $\tau_G = L/2V$, where L is the gust correlation distance, and V is the aircraft flight speed. A comparison of the von Kármán spectrum with the present approximation shows that the two spectra are quite close (ref. 10), as expected since both the low frequency level and the rms values have been matched. A correlation length of $L = 120$ m is used, which is typical of low altitude turbulence (ref. 11). For the gust strength σ_G, 2 m/sec is typical of clear air turbulence (CAT), and 6 m/sec for thunderstorms (refs. 12 and 13).

Finally, note that the gust model is based on Taylor's hypothesis, that for an aircraft flying with velocity V through a turbulence field in space, the gust spectrum with time frequency ω is obtained from the spectrum with space frequency Ω_x by the substitution $\omega = V\Omega_x$. It has been established that that this is a good model for turbulence, but it is not valid at $V = 0$. Thus we are not designing a controller for hover or very low speed operation of the proprotor aircraft (only speeds 40 knots and above are considered).

System Performance

To determine the control system performance, the open and closed loop dynamic stability are examined, in particular the damping ratio of the wing bending modes, which are the critical modes for proprotor dynamics. Furthermore we consider the rms response of the wing and rotor to aerodynamic gust excitation. The covariance matrix $X = E(xx^T)$ is obtained directly from the matrices in the equations of motion (ref. 9). The rms response is given per unit rms gust level. For the wind motion we examine the rms acceleration at the wing tip (vertical and chordwise) in g's per m/sec of gust velocity. For the rotor flap and lag motion we consider the rms response in the rotating frames, in degrees per m/sec of gust velocity. The response in the rotating frame is given by the square root of the sum of the squares of the response in the nonrotating frame. For example, the flap motion β is obtained from the gimbal pitch and yaw (β_{1c} and β_{1s}) by $\beta = .707\ (\beta_{1c}^2 + \beta_{1s}^2)^{1/2}$; the result for the cyclic lag motion (ζ) is similar. In general, this is simply a measure of the total cyclic flap and lag response.

RESULTS AND DISCUSSION

Operating State

Figure 1 shows the operating states considered for the gimballed proprotor: the schedule of rotor tip speed (ΩR), pylon angle (α_p), and thrust coefficient-solidity ratio (C_T/σ) as a function of flight speed. The resulting advance ratio μ (the component of forward velocity parallel to the disk plane, divided by the tip speed), and inflow ratio λ (normal velocity component divided by tip speed) are also shown. The entire range of tilting proprotor operation is covered, from 0 to 280 knots at sea level standard conditions. Helicopter forward flight extends up to 80 knots. The pylon is converted from vertical to horizontal for V = 80 to 140 knots. Then in airplane mode, V = 140 to 160 knots, the wing flaps are raised and the rotor speed reduced. Finally airplane mode cruise extends to 280 knots. This conversion path corresponds roughly to the center of the conversion corridor of a representative tilting proprotor aircraft. Additional details of the operating state, and a discussion of the open loop dynamics, are given in reference 6.

Proprotor Gust Response

Figure 2 shows the gust response of the proprotor and wing over the speed range from 40 to 280 knots. We shall first examine the uncontrolled response. The rms rotor flap response is a maximum in high speed cruise, reaching about .45 deg/m/sec. This compares well with calculations for the complete aircraft, which give .3 to .5 deg/m/sec for V = 200 to 260 knots (ref. 2). The rms gust strength is typically 6 m/sec in thunderstorms, and 2 m/sec in clear air turbulence (CAT). Thus the 3σ flap response in CAT is of the order 2.6°. The flap response is not a loads problem for a gimballed rotor (unless the gimbal stops are encountered), but the large rotor flapping is involved in the excitation of the rest of the system. The rms rotor lag response increases greatly with speed, to about .26 deg/m/sec here. This cyclic lag motion produces blade loads for the gimballed rotor, the response at high speed cruise corresponding to the rotor design limit loads typically (ref. 1).

The wing tip vertical acceleration increases greatly with speed, to about .4 g/m/sec. This compares with about .2 g/m/sec calculated for the vertical acceleration at the crew station due to vertical gusts with a complete aircraft model (ref. 2). The trend with speed is similar for the cantilever wing and complete aircraft calculations, with a gust alleviation factor of about 2 for the crew station acceleration compared with the wind tip acceleration (note however that the former was calculated for a 3000 m altitude, and a gust correlation length of L = 300 m). Figure 2 gives a 3σ wing tip vertical acceleration in CAT of 2.4g at maximum speed, which is very high. The wing tip chordwise acceleration is low in helicopter mode, increases in conversion (due to the response to rotor thrust perturbations), and is roughly constant in airplane mode. Figure 2 gives about .12 g/m/sec, compared to about .07 g/m/sec for the crew station longitudinal acceleration response to longitudinal gusts with a complete aircraft model (ref. 2). The 3σ wing tip chordwise acceleration in CAT is then of the order .7g.

Optimal Deterministic Controller

Figure 2 compares the gust response for the proprotor and wing uncontrolled and with the optimal deterministic controller. The control system accomplishes a substantial reduction in the gust response. At maximum speed the closed loop flap and lag response is about 5% of the open loop response, and the wing tip acceleration is reduced to about 10% of the open loop level. The 3σ flap response in CAT is of the order $0.1°$, and the wing tip vertical acceleration 0.3g. Note that the gust response of the controlled system is relatively independent of speed, in contrast to the large increases with V for the loop response. Figure 2 also shows the damping ratio of the wing vertical bending mode. The wing modes are an important factor in the proprotor gust response. Their natural frequencies are fairly high compared to the gust frequencies, but the resonant response is high because of the very low damping (ref. 14). Hence the control system greatly increases the wing mode dynamic stability in order to reduce the gust response.

The wing flaperon control motion required increases roughly linearly with speed, as the flaperon aerodynamic effectiveness increases, to about .18 deg/m/sec at maximum speed. The rotor collective pitch control required is around .2 to .3 deg/m/sec over the entire speed range. The cyclic control increases with speed in helicopter and conversion modes, and is nearly constant in airplane mode at about .22 deg/m/sec. Thus the 3σ flaperon and rotor control required in CAT is of the order of $1.2°$, which is a reasonable level.

The implementation of the optimal controller would require that the feedback gains be programmed with the proprotor operating state, since a different control system is designed for each condition. It is preferable to use a single controller over the entire operating range. There are large changes in the open loop dynamics however, due to the variations of the flight speed, rotor speed, and especially pylon angle; hence it is not necessarily expected that a single controller will be feasible. Figure 2 also shows the closed loop gust response using a single controller designed for optimal response at 160 knots. It is observed that nearly the same performance is achieved with this single controller as with the optimal controller for each speed — even in conversion mode where the pylon angle is changing. There is some degradation in the performance at low speed in helicopter mode however; for example, the wing chordwise bending mode damping (not shown) is actually reduced at 40 knots. We are not designing a controller for hover and very low speed anyway of course. If necessary the controller could probably be programmed with the pylon angle without too much difficulty.

The controller designed by this process is not simple. The state variable feedback matrix C has 84 elements (18 states, 3 gust components, and 4 controls). While many of the elements are negligibly small, the remaining feedback loops comprise a fairly sophisticated system. For example, for the 160 knot controller the major loops are: ψ_g, $\dot{\psi}_g$, rotor coning, wing motion and wing velocity feedback to rotor collective; rotor flap and lag motion, flap and lag velocity, wing motion and wing velocity feedback to rotor cyclic; and wing vertical bending velocity feedback to wing flaperon. There are two particularly notable loops. The wing flaperon control is almost entirely

feedback of the wing velocity: $\delta_F = -Kq_{w_l}$. The wing lift due to the flaperon is directly responsible for the large increase in the wing vertical bending mode damping. The other loop is the ψ_s feedback to collective pitch, which is essentially a very tight governor on the rotor speed: $\theta_o = K_I\psi_s + K_p\dot{\psi}_s$. The integral gain K_I equals 18.8 deg/sec/rpm over the entire speed range, which is very high (0.1 to 0.5 deg/sec/rpm would be typical of a governor designed for power management). The lead in the network is small, K_p/K_I = .03 to .10 sec. Essentially this loop eliminates the rotor speed perturbations from the dynamics, which has a general stabilizing influence (ref. 6).

Gain Sweeps

Figures 3 and 4 present the wing tip vertical acceleration, wing vertical bending mode damping ratio, and rotor flap response for a gain sweep at V = 240 knots (in airplane cruise mode). Increasing the gain decreases the weight in the performance index on the control motions compared to the rotor and wing motions, thus producing tighter control. The results of figure 2 were for a gain = 10, which we see achieves most of the gust response reduction possible (with this particular design process and performance index). The only significant improvement with higher gain is a lower wing vertical acceleration response. Above a gain = 10 there is little increase in the rotor control motion, so most of the improvement at higher gain is due to a larger wing flaperon control motion (which increases roughly linearly with gain).

Figures 3 and 4 compare the controlled response with and without the wing flaperon control, demonstrating the important role of this control in the gust alleviation system. Without the flaperon control, a closed loop wing tip vertical acceleration response of only .085 g/m/sec is achieved (3σ response in CAT order .5g). The wing flaperon allows a substantially greater reduction in the wing response, and also allows the rotor controls to reduce the rotor response more. The wing vertical bending mode achieves only about 12% critical damping without the flaperon control. The flaperon allows a direct, powerful control of the wing vertical bending mode, which has a central role in the proprotor dynamic stability and gust response. The effectiveness of such a control surface would certainly require experimental verification, for it depends on viscous, unsteady, and three-dimensional aerodynamic effects; and on the structural limitations to the flap oscillations. It is concluded though that the wing flaperon should definitely be included in the controller design.

Now let us examine the control system design considering only part of the system. Figure 3 shows the wing response for an optimal controller designed with performance index weights on the rotor motion only (and with no flaperon control either). The closed loop gust response of the rotor (not shown) remains satisfactory; it is even somewhat smaller than with the performance index constraint on all degrees of freedom. There is a moderate reduction in the wing motion still, since much of the rotor response is due to the wing motion. The 30% reduction (to .10 g/m/sec) in wing tip vertical acceleration achieved is not satisfactory performance however. Moreover, the damping ratio of the wing vertical bending mode is actually decreased by the control system

when the wing motion is not considered in the design (fig. 3). Such a dynamic stability degradation is not acceptable. Such behavior of a control system designed considering the rotor alone has been observed in full-scale tests of a proprotor and a cantilever wing (ref. 15). Figure 5 (from ref. 15) shows the performance obtained with integral feedback of the longitudinal flapping to longitudinal cyclic ($\dot{\theta}_{1s} = -K\beta_{1c}$). A substantial reduction of the transient flapping is achieved, but at the expense of increased wing vertical bending motion (the transient motion was obtained by step cyclic control inputs). With integral feedback, the steady state flap response was zero, and increasing the gain improved the transient flap dynamics (with reduced flap damping however). The increased wing response for the uncompensated network was unacceptable however, and the wing vertical bending mode damping (not shown) was decreased also, with an unstable point at a gain of 5 for 265 knots. Lagged position feedback of the rotor flapping was also tried. This loop was somewhat more effective than the integral network in reducing the transient flapping, but produced more wing response; there was also a reduction in stability with gain. With a combination of integral and lagged position feedback, a reduction in transient flapping of about 30% was achieved with only a small damping reduction and increase in wing motion (combinations were also found with worse performance).

Alternatively, we may examine the control system design with only the wing motion considered. Figure 4 shows the rotor flapping response as a function of gain for an optimal controller designed with performance index weights on the wing motion only (and no flaperon control again). The resulting controller has virtually no feedback of the rotor degrees of freedom. The wing response and damping (not shown) remain satisfactory; a damping ratio of the wing vertical bending mode above 30% critical is achieved even with no flaperon control. The rotor response however is unacceptable. The flap response at high gain is even larger than open loop. The behavior of the cyclic lag motion, hence the blade loads, is similar.

It is concluded that a satisfactory controller design requires a consideration of the complete dynamic system, not just the motion of the wing or the rotor alone. Relaxing the constraint on part of the system allows only a small improvement in the response of the rest, which does not compensate for the deterioration of the dynamic behavior of the unconstrained motions. The optimal control analysis provides a means to design controllers considering the entire system, both rotor and support, although the resulting designs are by no means simple.

Measurements

We have found that the optimal controller is linear state feedback, with major loops involving almost all the degrees of freedom of the system. As an alternative to measuring all the degrees of freedom, let us consider the use of a compensation network to estimate the system states from a limited number of measurements. A Kalman-Bucy filter is used for the compensation network. The question is what measurements are required to satisfactorily control the system. Figure 6 shows the rotor flap and wing tip vertical acceleration gust

response for various measurements, to be compared with the open loop and optimally controlled results of figure 2. Without a measurement of the rotor rotational speed perturbation ($\dot{\psi}_s$), satisfactory control is not generally possible (the closed loop response can be degraded so far as to be larger than open loop even). The important role of ψ_s in the proprotor dynamics and control has been pointed out. Since the rotor behaves nearly as if windmilling, an accurate estimate of the rotational speed perturbations from the motion of the other degrees of freedom is not possible. It is necessary to measure ψ_s directly. Figure 6 shows that the flap response remains high with measurements of the wing motion and the rotor speed perturbation only. It is necessary to also measure the rotor flap motion (β, i.e., gimbal pitch and yaw) to achieve satisfactory control of both the wing and rotor motions. Adding measurements of the rotor coning and lag motion (β_o, ζ), which must be obtained in the rotating frame, does not improve the performance much; certainly not enough in view of the great difficulties in obtaining such measurements. The rotor tip-path-plane tilt for the gimballed rotor may be measured in the nonrotating frame however.

It is observed in figure 6 that by measuring the wing motion and the gust velocities, i.e., the disturbances which are exciting the system, the gust response may be reduced nearly to the level obtained with perfect knowledge of the states. (Performance almost this good can be obtained by measuring only the gust velocities in fact.) Measuring the excitation is therefore a very efficient means to estimate the states and thus achieve nearly the optimum controller performance. It is assumed of course that the model of the rotor, support, and gust dynamics used in the Kalman-Bucy filter is an accurate representation of the real system. Errors in the model will degrade the performance.

In summary, a compensation network may be used to reduce the measurements required for the proprotor gust alleviation control system. The measurements required for satisfactory control are the wing motion, the rotor rotational speed perturbation, and the rotor tip-path-plane tilt. Measurements in the rotating frame are thus not really required for a gimballed proprotor. An excellent source of information is the measurement of the exciting gust velocity itself, assuming that an accurate model is available to estimate the states from the excitation. The compensation network we have used, a Kalman-Bucy filter, is certainly not simple of course. It is also noted that the filter tends to be more sensitive than the deterministic controller to off-design operation and to errors in the system model.

Antisymmetric Dynamics

A major difference between the symmetric and antisymmetric dynamics of the proprotor aircraft is the effect of the interconnect shaft on the antisymmetric motions (refs. 2 and 5). The interconnect shaft introduces a strong spring on the rotor azimuth perturbation, so the ψ_s root becomes an oscillatory mode with a frequency above .5/rev. The spring changes the phase of ψ_s relative to the wing motions, with a substantial impact on the dynamic stability and gust response (the wing vertical bending mode is stabilized, and

the chordwise mode destabilized). The antisymmetric dynamics may be represented with the proprotor and cantilever wing model by simply including the interconnect shaft spring. The open loop gust response for antisymmetric motions is close to that for symmetric motions; the only significant difference is about 25% lower wing tip vertical acceleration, due to the higher damping of that motion. The 3σ response of the wing tip vertical acceleration in CAT is of the order 1.8g at max speed. The closed loop (optimal controller) gust response is virtually identical for the symmetric and antisymmetric motions.

The major difference between the symmetric and antisymmetric motions is that for the latter the rotor azimuth perturbations result in interconnect shaft and drive train loads, which may be significant. Indeed, for a typical proprotor aircraft, design limit drive train loads are encountered due to antisymmetric longitudinal gusts in cruise mode. Figure 7 shows the gust response of the rotor azimuth perturbation for the case of antisymmetric motion and gusts. The open loop response increases to .3 deg/m/sec at maximum speed, which we may consider a measure of the design limit loads. The optimal controller produces a gust response which varies little with speed, and is about 15% of the uncontrolled level at maximum speed.

Hingeless Rotor

To examine the influence of the rotor type on the proprotor gust response and control, we also consider a hingeless, soft-inplane proprotor. A complete description of the rotor is given in reference 6. The rotor has three blades, and a radius of 3.96 m. The flap frequency is approximately $\nu_\beta = 1.35$/rev in cruise mode, and the lag frequency $\nu_\zeta = .75$/rev (the flap frequency is somewhat lower in helicopter mode because of the higher rotor speed). The uncontrolled dynamics of the hingeless proprotor are discussed in reference 6. There are major differences compared with the open loop dynamics of the gimballed rotor, due to the placement of the natural frequencies of the blade flap and lag motions. It is found however that the controlled dynamics and gust response of the gimballed and hingeless rotors are very similar, because for high gain it is the feedback loop which determines the system characteristics. A detailed, parallel study of hingeless and gimballed proprotor gust response and alleviation is given in reference 14.

Figure 8 shows the rms rotor lag and wing tip vertical acceleration response to gust, for the uncontrolled and optimally controlled system. The flap response is similar to the lag response, but smaller; the two blade motions give about the same blade loads for this rotor, so the lag response is critical. The 3σ response of the rotor lag motion in CAT is of the order 3.2°, which is quite high. The rotor response is reduced to about 10% of the open loop value by the optimal controller. The 3σ response of the wing tip vertical acceleration in CAT is of the order 1.3g, which is reduced to about .2g by the control system. Figure 8 also shows the gust response using a Kalman-Bucy filter to estimate the states from various measurements. As for the gimballed rotor, it is concluded that it is necessary to measure the wing motion, the rotor speed perturbation, and the rotor tip-path-plane tilt for adequate performance of the control system. Measurements of the rotor coning

and cyclic lag motion are still not required. To obtain the tip-path-plane measurement for a hingeless rotor, either the hub moment must be measured in the nonrotating frame, or the blade root bending in the rotating frame. Neither measurement is easily obtained, so the practical implementation of the control system is more difficult than for the gimballed rotor. The alternative of measuring the gust velocities to estimate the states indirectly from the excitation is more attractive for the hingeless rotor therefore, and thus the accuracy of the rotor, support, and gust models becomes a more important factor.

CONCLUDING REMARKS

From this optimal control investigation, it is concluded that a substantial improvement in the tilting proprotor gust response is possible with a properly designed controller, including improved ride quality, reduced rotor loads and motion, reduced pylon vibration, reduced drive-train loads, and improved dynamic stability. The state variable feedback designed here is not simple however, involving feedback of almost all the wing and rotor states. We have demonstrated the importance of considering the entire system in the controller design, not just the rotor or wing alone; and the usefulness of the wing flaperon control in a gust alleviation system for proprotor aircraft. Efficient control requires the measurement of the wing motion, the rotor speed perturbation, and the tip-path-plane tilt. The only real difficulty is with the measurement of the tip-path-plane tilt or hub moment for a hingeless rotor. An alternative is to measure the exciting disturbance, from which a very good estimate of the states may be obtained if an accurate model of the system is available. Finally, it was found that a single controller operated efficiently over the entire speed range, even though it is nominally optimal only for the design point (160 knots). The gust alleviation system may however require programming with nacelle tilt or speed because of some degradation in performance at very low speed; but the design of controllers for hover has not been considered at all.

The next steps in the investigation are fairly clear. A complete model of the tilting proprotor aircraft, including the rigid body modes and a detailed control system model, is required to proceed. Two major areas still to be examined are the design of a controller for gust alleviation in hover and very low speed, and the influence of the gust alleviation system on the aircraft handling qualities. Then we may consider the design of a practical gust alleviation control system for actual tilting proprotor aircraft, to be tested in the wind tunnel and flight.

REFERENCES

1. Gaffey, T. M., Yen, J. G., and Kvaternik, R. G., "Analysis and Model Tests of the Proprotor Dynamics of a Tilt-Proprotor VTOL Aircraft," U.S. Air Force V/STOL Technology and Planning Conference, Las Vegas, Nevada, September 1969

2. Anon., "V/STOL Tilt-Rotor Study — Research Aircraft Design," Bell Helicopter Company, NASA CR 114442, June 1972

3. DeTore, J. A., and Sambell, K. W., "Conceptual Design Study of 1985 Commercial Tilt Rotor Transports," NASA CR 2544, November 1974

4. Johnson, Wayne, "Analytical Model for Tilting Proprotor Aircraft Dynamics, Including Blade Torsion and Coupled Bending Modes, and Conversion Mode Operation," NASA TM X-62,369, August 1974

5. Johnson, Wayne, "The Influence of Engine/Transmission/Governor on Tilting Proprotor Aircraft Dynamics," NASA TM X-62,455, June 1975

6. Johnson, Wayne, "Analytical Modeling Requirements for Tilting Proprotor Aircraft Dynamics," NASA TN D-8013, July 1975

7. Bryson, Arthur E., Jr., and Ho, Yu-Chi, *Applied Optimal Control*, Blaisdell Publishing Co., Waltham, Massachusetts, 1969

8. Anderson, Brian D. O., and Moore, John B., *Linear Optimal Control*, Prentice-Hall, Inc., Englewood Cliffs, New Jersey, 1971

9. Hall, W. E., Jr., and Bryson, A. E., Jr., "Inclusion of Rotor Dynamics in Controller Design for Helicopter," J. Aircraft, vol. 10, no. 4, April 1973

10. Gaonkar, Gopal H., and Hohenemser, Kurt H., "Stochastic Properties of Turbulence Excited Rotor Blade Vibrations," AIAA Journal, vol. 9, no. 3, March 1971

11. Gault, J. D., and Gunter, D. E., Jr., "Atmospheric Turbulence Considerations for Future Aircraft Designed to Operate at Low Altitudes," J. Aircraft, vol. 5, no. 6, November-December 1968

12. Houbolt, John C., Steiner, Roy, and Platt, Kermit G., "Dynamic Response of Airplanes to Atmospheric Turbulence Including Flight Data on Input and Response," NASA TR R-199, June 1964

13. Anon., "Military Specification, Flying Qualities of Piloted Airplanes," MIL-F-8785B(ASG), U.S. Air Force, August 1969

14. Frick, Juanita K., and Johnson, Wayne, "Optimal Control Theory Investigation of Proprotor/Wing Response to Vertical Gust," NASA TM X-62,384, September 1974

15. Anon., "Advancement of Proprotor Technology — Wind-Tunnel Test Results," Bell Helicopter Company, NASA CR 114363, September 1971

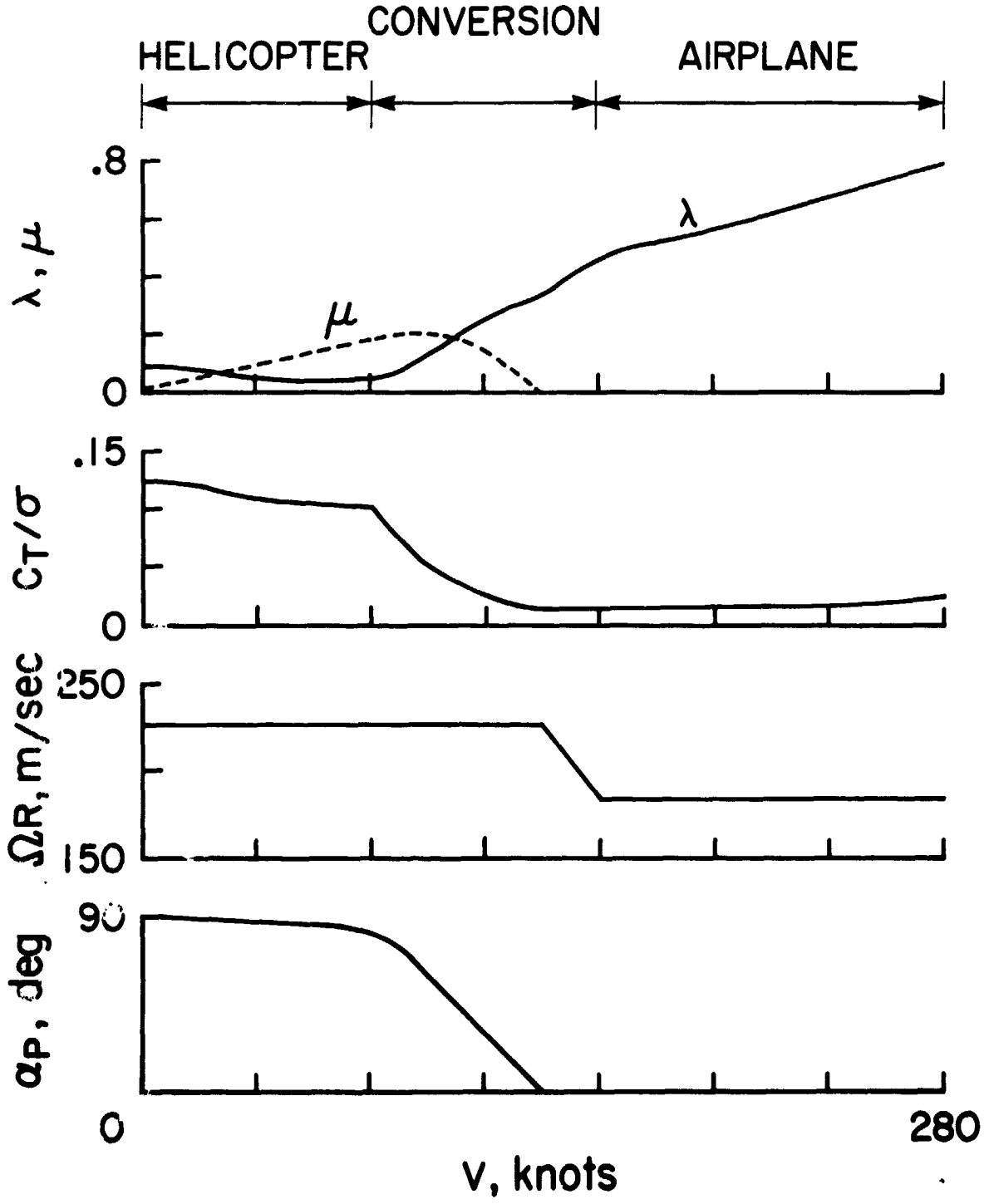

Figure 1.- Gimballed proprotor operating state: inflow ratio, advance ratio, thrust, tip speed, and pylon angle schedule with forward speed.

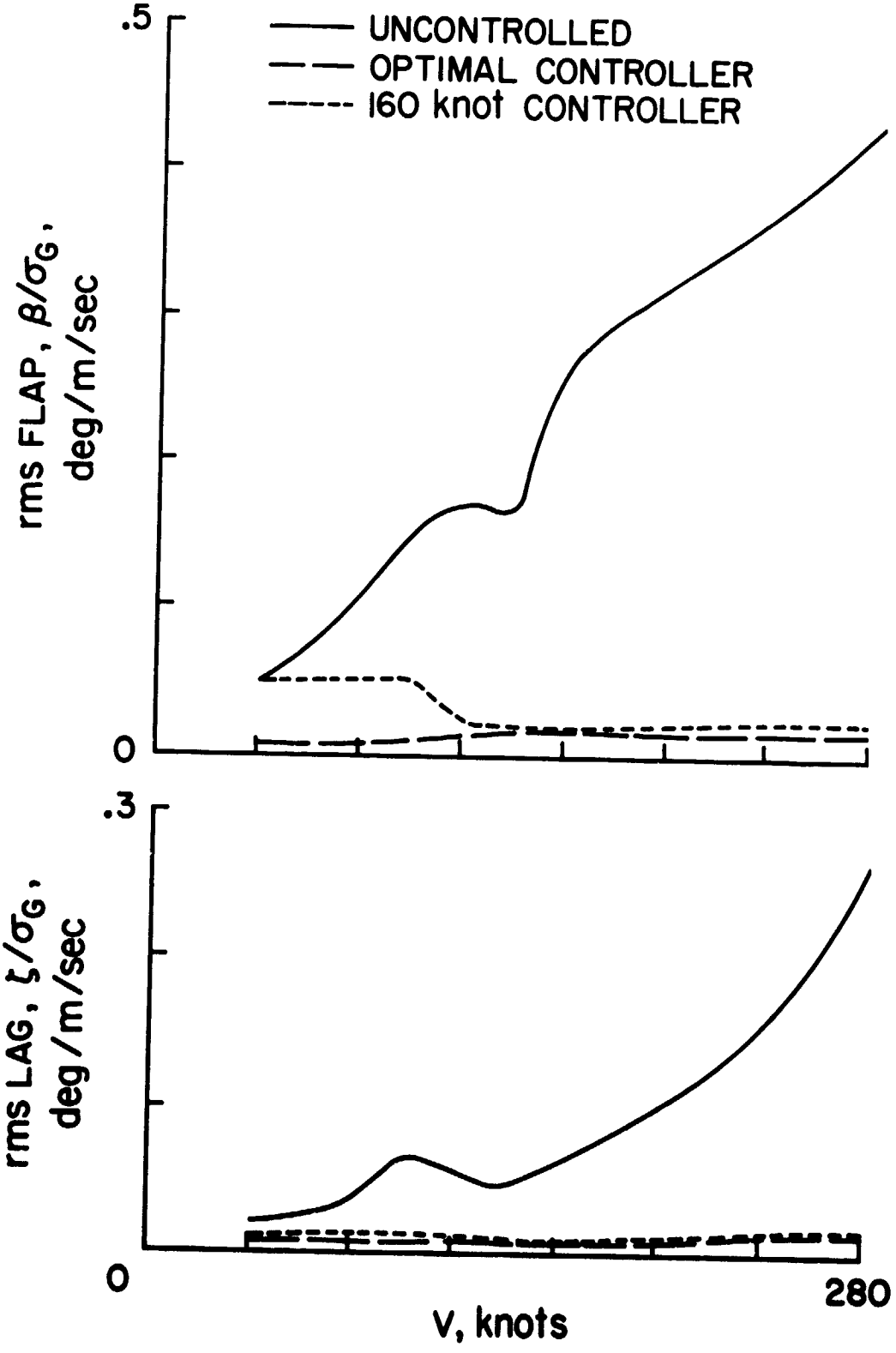

Figure 2.- Gimballed proprotor and wing gust response uncontrolled, with optimal controller, and with 160 knot controller. Rms flap and lag motion per rms gust velocity, rms wing tip vertical and chordwise acceleration, and wing vertical bending mode damping ratio.

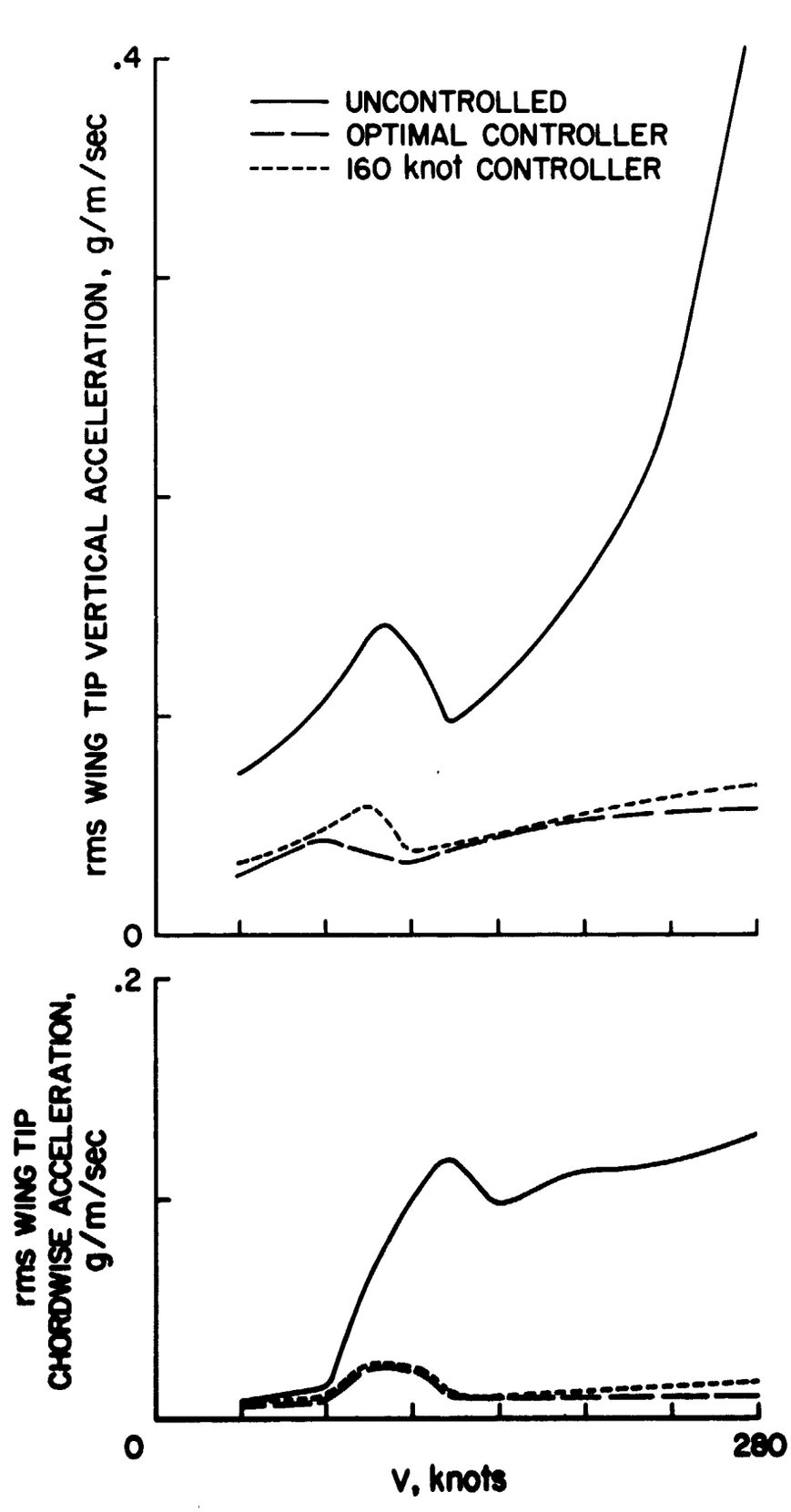

Figure 2.- Continued.

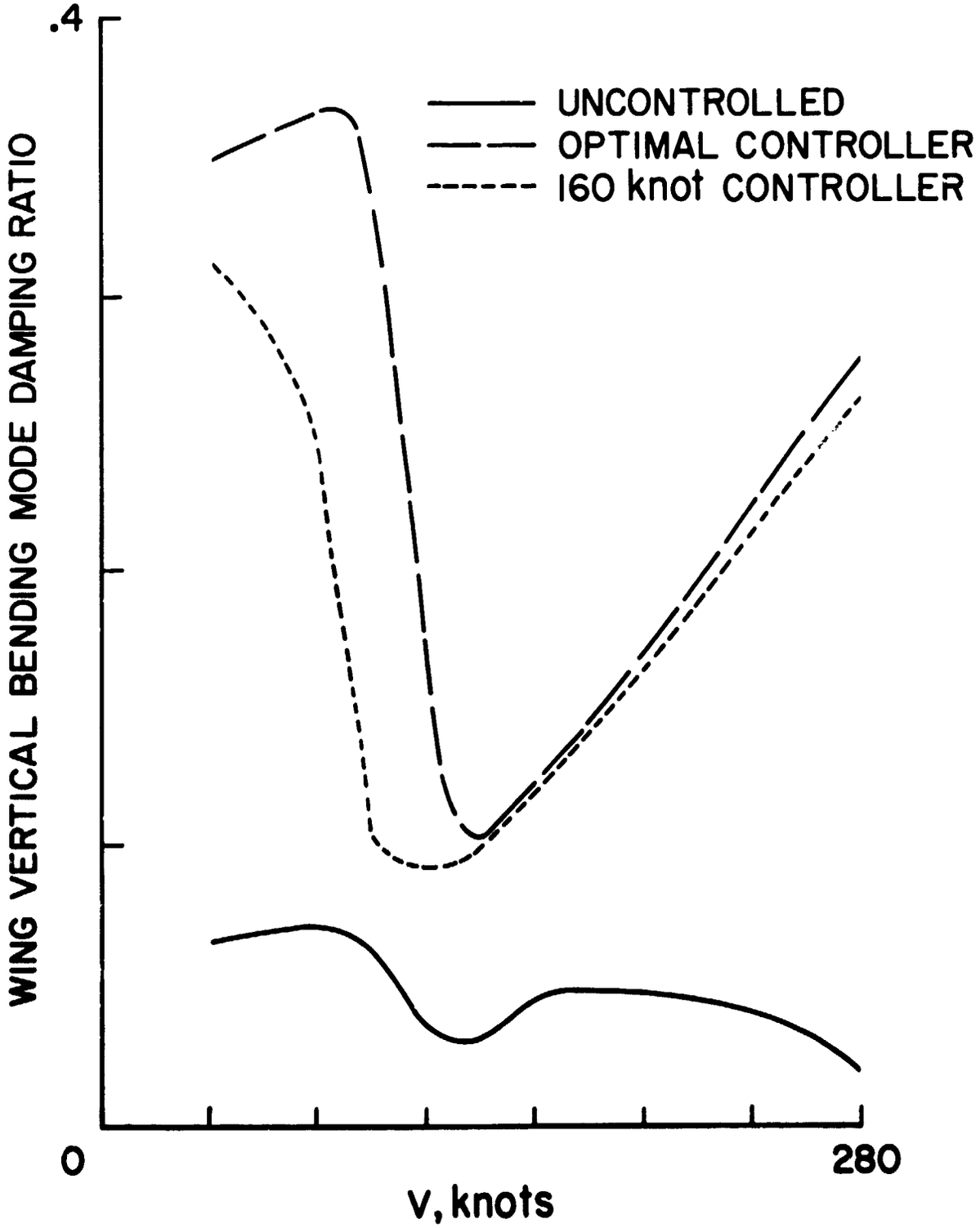

Figure 2.- Concluded.

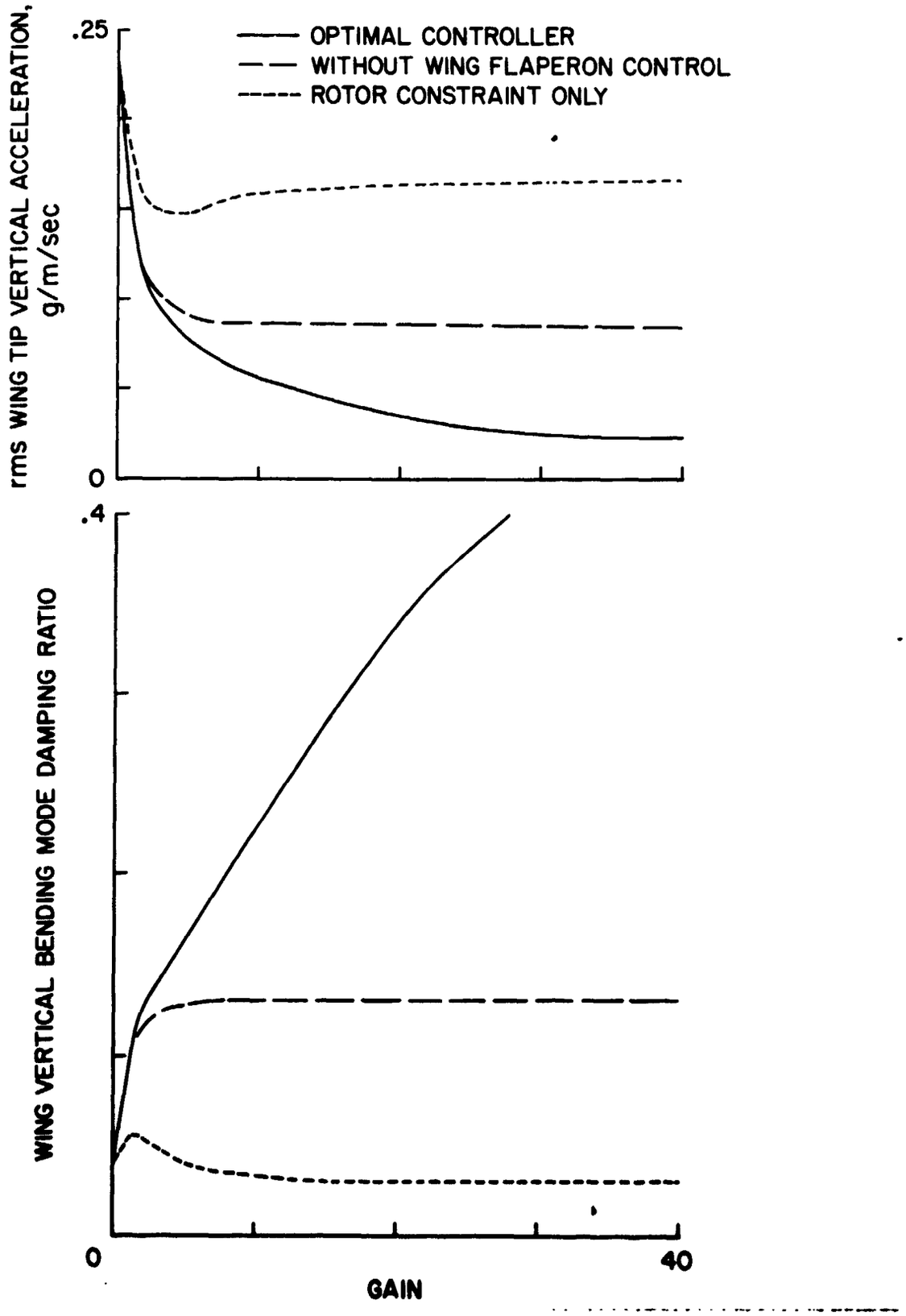

Figure 3.- Wing tip vertical acceleration and wing vertical bending mode damping ratio at 240 knots, showing the influence of the wing flaperon control, and the effect of designing optimal controller with constraint on the rotor motion only.

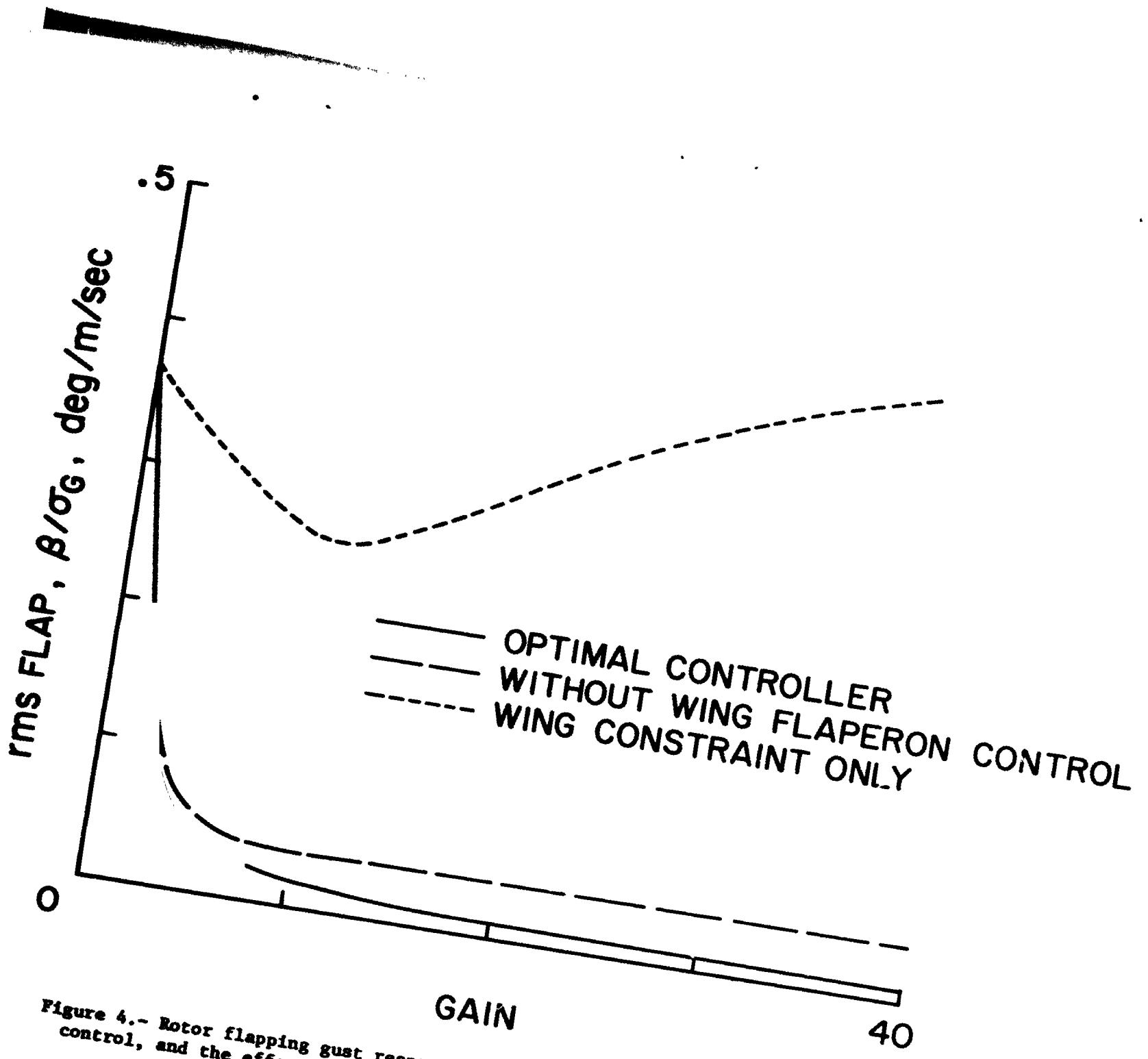

Figure 4.- Rotor flapping gust response at 240 knots, showing the influence of the wing flaperon control, and the effect of designing optimal controller with constraint on wing motion only.

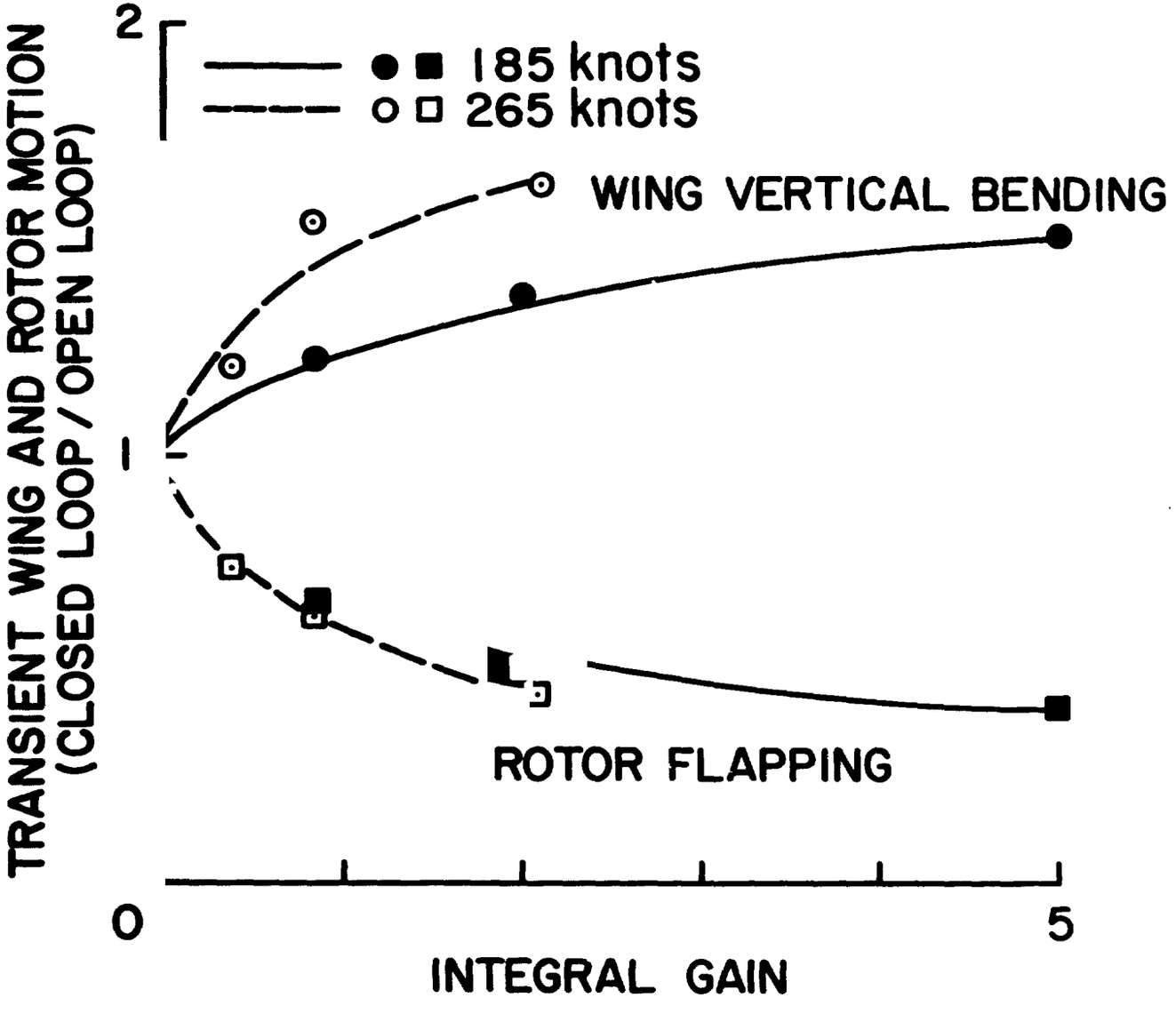

Figure 5.- Full-scale test results for ratio of closed-loop to open-loop transient response of rotor and wing motion, as a function of integral gain.

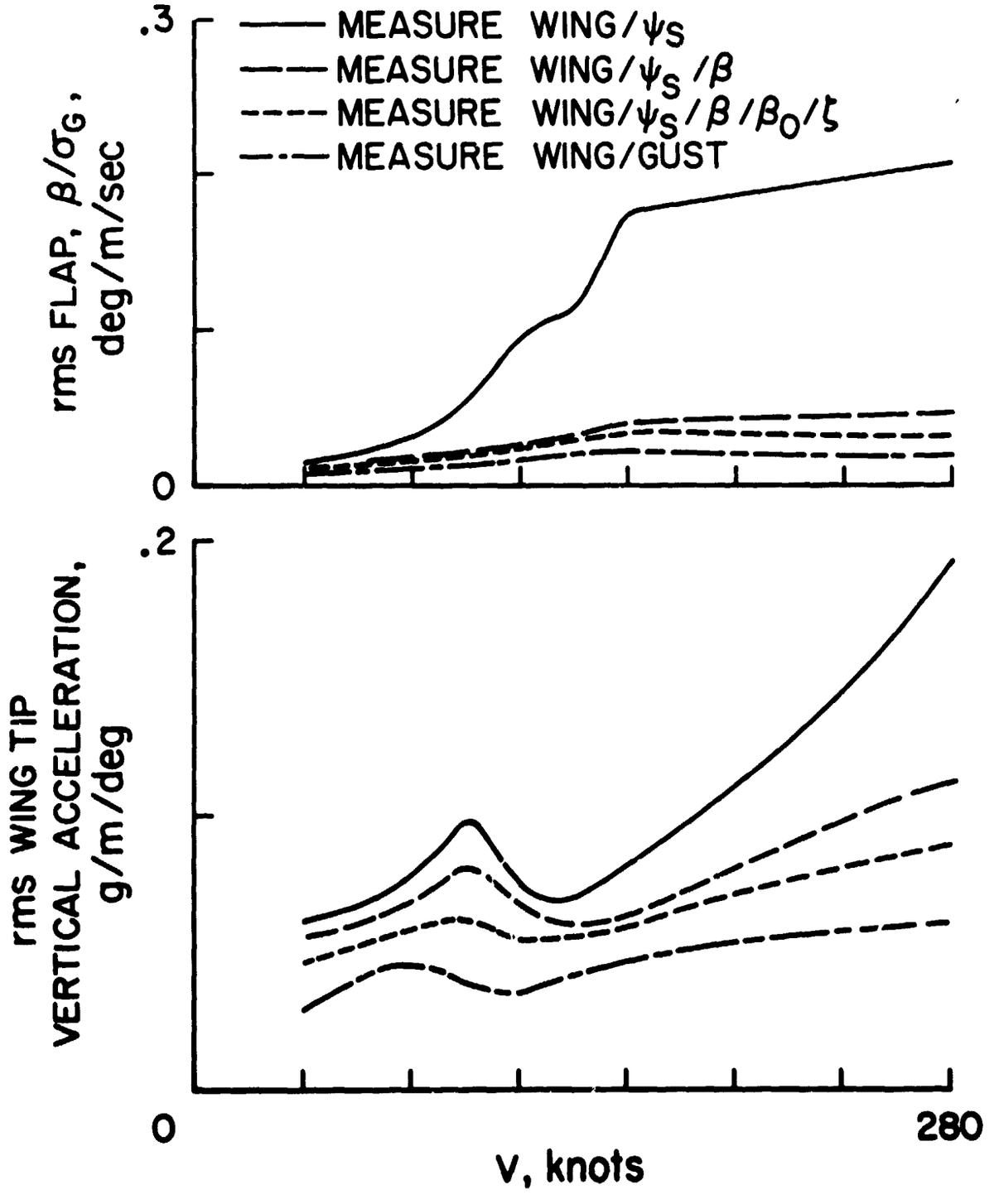

Figure 6.- Rotor flap and wing tip vertical acceleration gust response for controller with states estimated from various measurements in system.

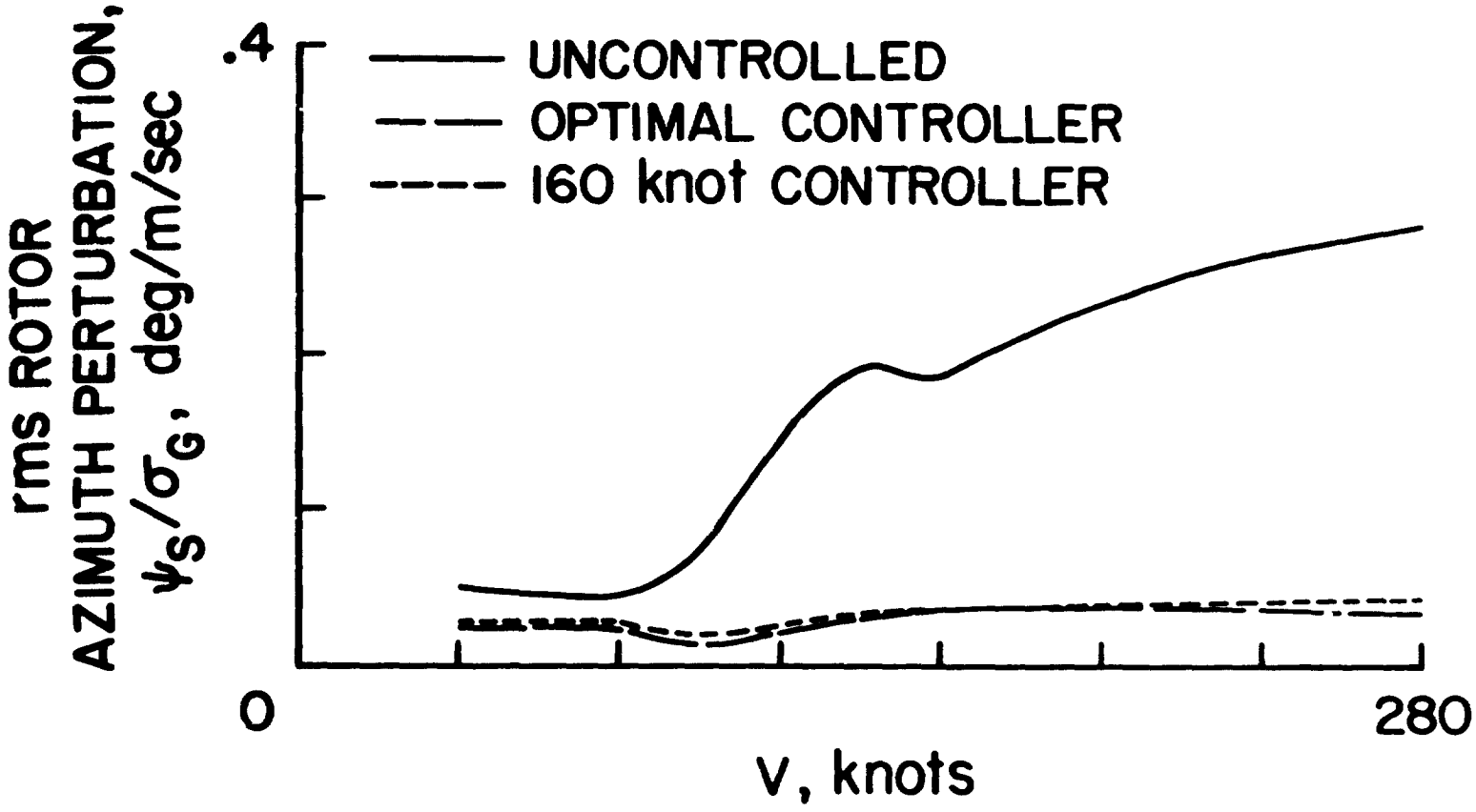

Figure 7.- Gust response of rotor azimuth perturbation for antisymmetric motion of gimballed proprotor and wing.

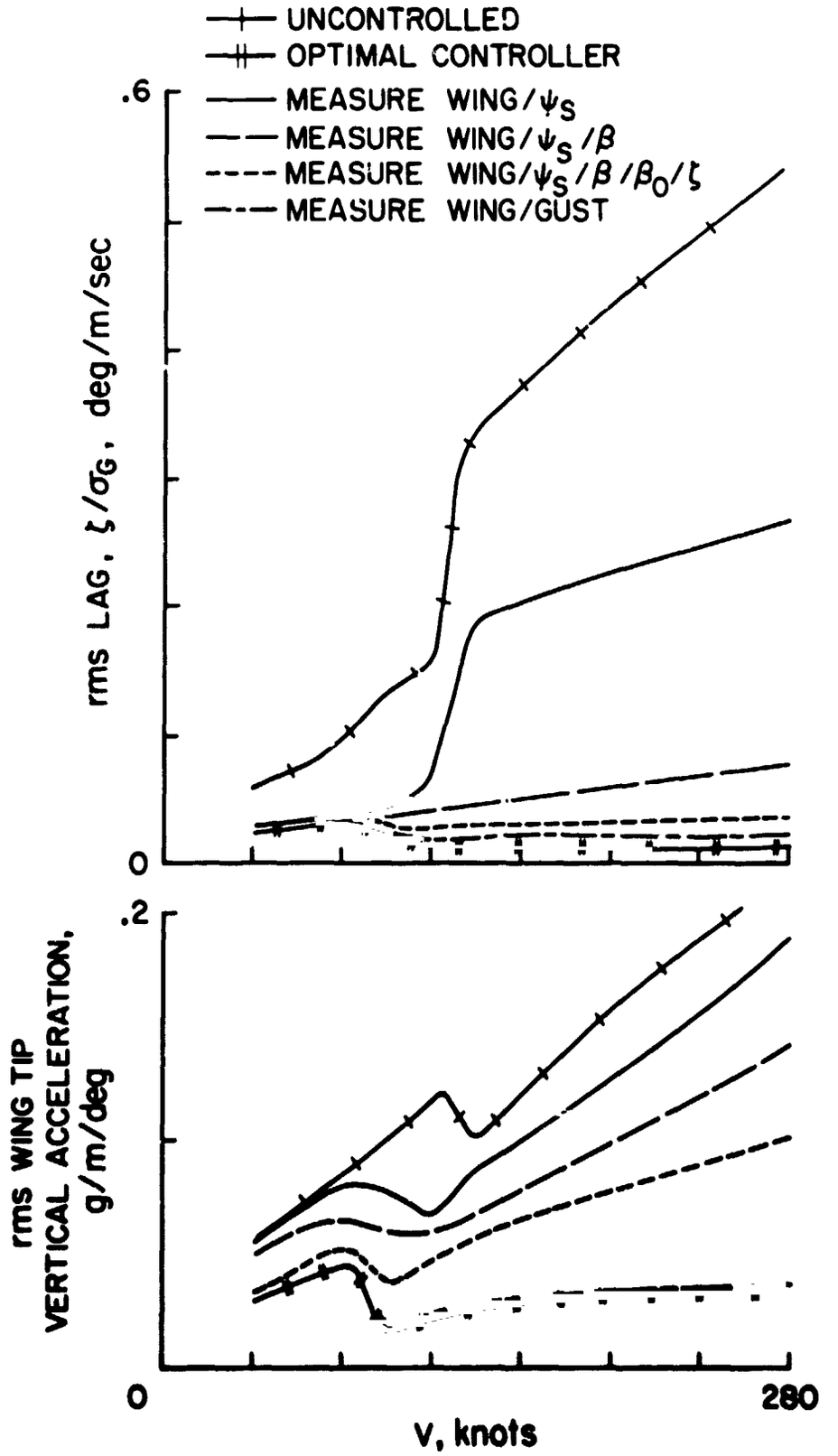

Figure 8.- Hingeless proprotor and wing gust response (rotor lag motion and wing tip vertical acceleration) uncontrolled, and with optimal deterministic controller. Also shown is the controlled response with states estimated from various measurements.